J|A|C|S
ARTICLES
Published on Web 01/25/2003

Side Chain Dynamics in Unfolded Protein States: an NMR Based ^{2}H Spin Relaxation Study of Δ131Δ

Wing-Yiu Choy,[†] David Shortle,[‡] and Lewis E. Kay*,[†]

Contribution from The Protein Engineering Network Center of Excellence and Departments of Medical Genetics and Microbiology, Biochemistry, and Chemistry, University of Toronto, Toronto, Ontario, Canada M5S 1A8 and Department of Biological Chemistry, The Johns Hopkins University School of Medicine, Baltimore, Maryland 21205

Received September 13, 2002; Revised Manuscript Received October 31, 2002; E-mail: kay@pound.med.utoronto.ca.

Abstract: NMR relaxation data on disordered proteins can provide insight into both structural and dynamic properties of these molecules. Because of chemical shift degeneracy in correlation spectra, detailed site-specific analyses of side chain dynamics have not been possible. Here, we present new experiments for the measurement of side chain dynamics in methyl-containing residues in unfolded protein states. The pulse schemes are similar to recently proposed methods for measuring deuterium spin relaxation rates in $^{13}CH_2D$ methyl groups in folded proteins.[1] However, because resolution in $^1H-^{13}C$ correlation maps of unfolded proteins is limiting, relaxation data are recorded as a series of $^1H-^{15}N$ spectra. The methodology is illustrated with an application to the study of side chain dynamics in Δ131Δ, a large disordered fragment of staphylococcal nuclease containing residues 1−3 and 13−140 of the wide-type protein. A good correlation between the order parameters of the symmetry axes of the methyl groups and the backbone $^1H-^{15}N$ bond vectors of the same residue is observed. Simulations establish that such a correlation is only possible if the unfolded state is comprised of an ensemble of structures which are not equiprobable. A motional model, which combines wobbling-in-a-cone and Gaussian axial fluctuations, is proposed to estimate χ_1 torsion angle fluctuations, σ_{χ_1}, of Val and Thr residues on the basis of the backbone and side chain order parameters. Values of σ_{χ_1} are approximately 10° larger than what has previously been observed in folded proteins. Of interest, the value of σ_{χ_1} for Val 104 is considerably smaller than for other Val or Thr residues, suggesting that it may be part of a hydrophobic cluster. Notably large ^{15}N transverse relaxation rates are observed in this region. To our knowledge, this is the first time that side chain dynamics in an unfolded state have been studied in detail by NMR.

Introduction

Early views of the relation between protein structure and function were based on the notion that proteins lacking stable secondary and tertiary interactions would not be able to perform their biological functions. This idea, however, has been challenged in the past several years by the results of many studies, which show that some proteins are biologically active despite the fact that they contain significant regions of disorder or, in some cases, lack discernible structure.[2−4] On the basis of the results of amino acid sequence analyses and neural network techniques, Dunker and co-workers have predicted that a significant fraction of protein sequences in various genomes may code for disordered proteins.[5] Recent studies of a number of such proteins have led to the suggestion that conformational disorder may play an important role in both the diversity of biomolecular interactions and the rapid turnover of important regulatory molecules.[2,3] The characterization of the structure and dynamics of unfolded proteins has thus become crucial to understanding their function. Equally important, identification of structural and dynamical propensities of unfolded molecules may provide insight into the protein folding process.

NMR is one of the most powerful techniques for studying disordered states of proteins. Residual structure can be assessed from scalar *J*-coupling constants,[6−8] short-range NOEs,[9] as well as chemical shifts.[10,11] In addition, dynamic properties can be studied by spin relaxation measurements,[12−15] to obtain site-

[†] University of Toronto.
[‡] The Johns Hopkins University School of Medicine.

(1) Millet, O.; Muhandiram, D. R.; Skrynnikov, N. R.; Kay, L. E. *J. Am. Chem. Soc.* **2002**, *124*, 6439−6448.
(2) Dyson, H. J.; Wright, P. E. *Curr. Opin. Struct. Biol.* **2002**, *12*, 54−60.
(3) Wright, P. E.; Dyson, H. J. *J. Mol. Biol.* **1999**, *293*, 321−331.
(4) Uversky, V. N. *Pro. Sci.* **2002**, *11*, 739−756.
(5) Dunker, A. K.; Lawson, J. D.; Brown, C. J.; Williams, R. M.; Romero, P.; Oh, J. S.; Oldfield, C. J.; Campen, A. M.; Ratliff, C. M.; Hipps, K. W.; Ausio, J.; Nissen, M. S.; Reeves, R.; Kang, C. H.; Kissinger, C. R.; Bailey, R. W.; Griswold, M. D.; Chiu, W.; Garber, E. C.; Obradovic, Z. *J. Mol. Graphics Modell.* **2001**, *19*, 26−59.
(6) Serrano, L. *J. Mol. Biol.* **1995**, *254*, 322−333.
(7) Smith, L. J.; Bolin, K. A.; Schwalbe, H.; MacArthur, M. W.; Thornton, J. M.; Dobson, C. M. *J. Mol. Biol.* **1996**, *255*, 494−506.
(8) Fiebig, K. M.; Schwalbe, H.; Buck, M.; Smith, L. J.; Dobson, C. J. *J. Phys. Chem.* **1996**, *100*, 2661−2666.
(9) Dyson, H. J.; Wright, P. E. *Annu. Rev. Biophys. Biophys. Chem.* **1991**, *20*, 519−538.
(10) Wishart, D. S.; Sykes, B. D. *J. Biomol. NMR* **1994**, *4*, 171−180.
(11) Schwarzinger, S.; Kroon, G. J. A.; Foss, T. R.; Chung, J.; Wright, P. E.; Dyson, H. J. *J. Am. Chem. Soc.* **2001**, *123*, 2970−2978.
(12) Kay, L. E. *Nat. Struct. Biol.* **1998**, *NMR Suppl.*, 513−517.
(13) Palmer, A. G.; Kroenke, C. D.; Loria, J. P. *Methods Enzymol.* **2001**, *339*, 204−238.
(14) Palmer, A. G. *Annu. Rev. Biophys. Biomol. Struct.* **2001**, *30*, 129−155.

10.1021/ja021179b CCC: $25.00 **© 2003 American Chemical Society**

specific motional information, providing a qualitative measure of the interactions at each site.

Backbone ^{15}N amide relaxation measurements are commonly employed in the study of both folded and unfolded/disordered proteins.[15,16] Particularly important for applications to the study of unstructured protein states, where resolution in NMR spectra is critical, is the fact that ^{15}N chemical shifts in unfolded proteins are generally well dispersed. Dynamics information is thus available for many sites in the molecule. The picture that emerges from studies of a number of unfolded states is that the dynamics along the backbone are quite variable, with certain regions showing increased order, consistent with the formation of clusters of interacting residues.[17]

To further characterize the dynamics of such residues, it would be of interest to extend the backbone measurements described previously to include a study of motion at positions along the side chain. For example, the dynamics of methyl-bearing side chains can be used to probe the temporal nature of hydrophobic interactions in the core of proteins which is not forthcoming from studies of backbone spin relaxation. In the past several years, our laboratory has developed an approach for studying side chain dynamics in folded proteins in which ^2H spin relaxation rates are measured in ^{13}C-labeled, fractionally deuterated molecules.[1,18,19] Dynamics information is extracted on a per residue basis by recording a series of $^1H-^{13}C$ correlation spectra in which the intensities of the correlations encode the relaxation rate of interest. Order parameters characterizing the amplitudes of motions and correlation times describing their rates have been measured in a significant number of proteins and used to provide insight into the nature of molecular recognition[12,20−23] and protein stability.[24] Very recently, the ^2H spin relaxation methodology has been extended to include the measurement of five relaxation rates per deuteron[1] and applications to the study of the dynamics of methyl-containing side chains in the B1 domain of peptostreptococcal protein-L and in a mutant of the drkN SH3 domain[1,25] have appeared.

The investigation of side chain dynamics in unfolded protein states is, however, complicated by the fact that the resolution in $^{13}C-^1H$ correlation maps is poor and it is not possible to get residue specific dynamics information from such spectra. We have designed, therefore, a series of $^1H-\ ^{15}N$ correlation experiments in which magnetization encoding the methyl ^2H relaxation properties is transferred to the backbone amide for detection, facilitating the measurement of motional parameters on a per residue basis. The methodology is applied to a 131-residue fragment of staphylococcal nuclease (Δ131Δ), one of several model systems used to study unfolded states of proteins. Extensive structural characterization of this unfolded protein has been carried out using NMR and other spectroscopic techniques,[26−32] showing that Δ131Δ is relatively compact under nondenaturing conditions. ^2H relaxation rates have been measured at a large number of sites in the protein and used to estimate amplitudes of side chain dynamics using simple motional models. A strong correlation between order parameters at backbone and side chain positions is found which can only be explained by assuming that the unfolded state is comprised of an ensemble of molecules, with certain conformers much more probable than others.

Results and Discussion

Backbone ^{15}N Dynamics. A detailed backbone ^{15}N spin relaxation study has been reported by Alexandrescu and Shortle.[27] In this work, we have repeated these relaxation measurements so that backbone and side chain dynamics measured on the same protein sample can be compared. The profile of relaxation rates and NOE values as a function of residue is very similar to what has been published. Dynamics parameters were extracted from fits of the backbone relaxation data (R_1, $R_{1\rho}$, and $^1H-^{15}N$ NOE) using a spectral density function of the form[33,34]

$$J(\omega) = S_f^2 \frac{\tau_c^{eff}}{1+(\omega\tau_c^{eff})^2} + (1-S_f^2)\frac{\tau}{1+\omega^2\tau^2}, \qquad \frac{1}{\tau} = \frac{1}{\tau_c^{eff}} + \frac{1}{\tau_e} \quad (1)$$

where S_f is an order parameter which provides a measure of the amplitude of internal dynamics of the $^1H-^{15}N$ bond, τ_e is the correlation time of this motion, and τ_c^{eff} is a residue specific effective correlation time. The unfolded state of a protein is comprised of an ensemble of conformations which interconvert over a wide range of time scales. For example, in the case of Δ131Δ, the first 34 residues are not observed in $^1H-^{15}N$ correlation spectra recorded at 32 °C (see Materials and Methods) because of microsecond−millisecond time scale dynamics resulting from the formation of nascent structure. In contrast, other correlations are very intense, likely the result of interconversions that are fast on the NMR chemical shift time scale. Measured relaxation rates are, therefore, population weighted average quantities of the ensemble. It is clear that the dynamics of such a population are complex, and eq 1 is most certainly an oversimplification. In particular, the separation of the overall tumbling from internal dynamics becomes especially problematic in this case. Nevertheless, the small number of experimental observables coupled with our limited understanding of the nature of these dynamics at present precludes the use of more complex models. Relaxation data are well fit using the spectral density of eq 1 (χ^2 values less than 10^{-4}). Details and limitations of the approach are described in Yang et al.[35]

(15) Bracken, C. *J. Mol. Graphics Modell.* **2001**, *19*, 3−12.
(16) Kay, L. E.; Torchia, D. A.; Bax, A. *Biochemistry* **1989**, *28*, 8972−8979.
(17) Klein-Seetharaman, J.; Oikawa, M.; Grimshaw, S. B.; Wirmer, J.; Duchardt, E.; Ueda, T.; Imoto, T.; Smith, L. J.; Dobson, C. M.; Schwalbe, H. *Science* **2002**, *295*, 1719−1722.
(18) Muhandiram, D. R.; Yamazaki, T.; Sykes, B. D.; Kay, L. E. *J. Am. Chem. Soc.* **1995**, *117*, 11536−11544.
(19) Muhandiram, D. R.; Johnson, P. E.; Yang, D.; Zhang, O.; McIntosh, L. P.; Kay, L. E. *J. Biomol. NMR* **1997**, *10*, 283−288.
(20) Lee, A. L.; Kinnear, S. A.; Wand, A. J. *Nat. Struct. Biol.* **2000**, *7*, 72−77.
(21) Mittermaier, A.; Varani, L.; Muhandiram, D. R.; Kay, L. E.; Varani, G. *J. Mol. Biol.* **1999**, *294*, 967−979.
(22) Loh, A. P.; Pawley, N.; Nicholson, L. K.; Oswald, K. E. *Biochemistry* **2001**, *40*, 4590−4600.
(23) Ishima, R.; Louis, J. M.; Torchia, D. A. *J. Mol. Biol.* **2001**, *305*, 515−521.
(24) Lee, A. L.; Wand, A. J. *Nature* **2001**, *411*, 501−504.
(25) Skrynnikov, N. R.; Millet, O.; Kay, L. E. *J. Am. Chem. Soc.* **2002**, *124*, 6449−6460.
(26) Alexandrescu, A. T.; Abeygunawardana, C.; Shortle, D. *Biochemistry* **1994**, *33*, 1063−1072.
(27) Alexandrescu, A. T.; Shortle, D. *J. Mol. Biol.* **1994**, *242*, 527−546.
(28) Wang, Y.; Shortle, D. *Biochem.* **1995**, *34*, 15895−15905.
(29) Wang, Y.; Shortle, D. *Pro. Sci.* **1996**, *5*, 1898−1906.
(30) Gillespie, J. R.; Shortle, D. *J. Mol. Biol.* **1997**, *268*, 170−184.
(31) Gillespie, J. R.; Shortle, D. *J. Mol. Biol.* **1997**, *268*, 158−169.
(32) Ackerman, M. S.; Shortle, D. *Biochemistry* **2002**, *41*, 3089−3095.
(33) Lipari, G.; Szabo, A. *J. Am. Chem. Soc.* **1982**, *104*, 4546−4559.
(34) Lipari, G.; Szabo, A. *J. Am. Chem. Soc.* **1982**, *104*, 4559−4570.
(35) Yang, D.; Mok, Y. K.; Forman-Kay, J. D.; Farrow, N. A.; Kay, L. E. *J. Mol. Biol.* **1997**, *272*, 790−804.

and values of S_f^2, τ_e, and τ_c^{eff} are reported in the Supporting Information. It is worth noting that the effects of chemical exchange have been assessed by measuring $R_{1\rho}$ rates at three different B_1 fields[36] (1.1, 1.4, and 2.0 kHz); for the Val and Thr residues considered in what follows, the contributions of exchange to the extracted motional parameters are small (see later text).

Methyl Side Chain Dynamics. In a series of papers, we have described the use of ^{2}H spin relaxation to probe side chain dynamics in folded proteins.[1,12,18,19,25,37] The method selects $^{13}CH_2D$ methyls in ^{13}C-labeled, fractionally deuterated proteins and relaxation rates of the deuteron are measured indirectly in a series of ^{1}H−^{13}C correlation maps. As described previously, the situation is more complex for studies of unfolded proteins, since the very limited resolution in ^{1}H and ^{13}C dimensions precludes extracting site-specific data from spectra which record aliphatic chemical shifts. Thus, the magnetization transfer scheme used in the present experiments is

$$^1H_m \xrightarrow{J_{CH}} {}^{13}C_m \xrightarrow{J_{CD}} {}^{13}C_mD(T) \xrightarrow{J_{CD}} {}^{13}C_m \xrightarrow{J_{CC}} {}^{13}C_\alpha \xrightarrow{J_{C\alpha CO}} {}^{13}CO \xrightarrow{J_{CON}} {}^{15}N(t_1) \xrightarrow{J_{NH}} {}^1H(t_2) \quad (2)$$

where H_m and C_m denote methyl proton and carbon magnetization, respectively, D is the deuterium coherence of interest whose relaxation properties are measured during time T, $^{13}C_\alpha$ and ^{13}CO correspond to $^{13}C_\alpha$ and ^{13}CO magnetization of the methyl-containing residue, and ^{15}N and ^1H denote amide magnetization from the following amino acid. The couplings responsible for the transfer of magnetization are listed above the arrows in eq 2, and t_1 and t_2 denote acquisition times. A series of ^{1}H−^{15}N correlation maps are recorded as a function of delay T and the relaxation rate of the coherence of interest is measured from the decay of the signal. Figure 1 shows the sequences used to measure the decay of ^{2}H quadrupolar order, $3D_Z^2 - 2$ (a), and anti-phase transverse magnetization, $D_+D_Z + D_ZD_+$ (b). These experiments are very similar to ones that have recently appeared for the study of folded proteins,[1] and the interested reader is referred to the literature for further details. Related experiments for recording ^{2}H longitudinal and transverse relaxation rates in unfolded protein states have been published previously.[19]

^{2}H spin relaxation rates, corresponding to the decay of longitudinal (R_{D_Z}), transverse (R_{D_+}), and antiphase transverse ($R_{D_+D_Z+D_ZD_+}$) magnetization along with quadrupolar order ($R_{3D_Z^2-2}$), have been measured on an ^{15}N,^{13}C-labeled, fractionally deuterated Δ131Δ sample at two magnetic field strengths (500 and 600 MHz), 32 °C. In principle, a 5th relaxation rate corresponding to the decay of double quantum coherence could also be measured, as in our previous applications involving folded proteins,[1] although we have not done so in the present study. With the exclusion of residues in the β-meander (1−43) which are not observed in spectra of Δ131Δ[27] (except residues 1 and 2), there are 29 methyl-bearing residues in the protein (10 Ala, 3 Ile, 5 Leu, 4 Thr, and 7 Val). Figure 2 shows a two-dimensional ^{1}H−^{15}N spectrum (600 MHz) of amides from residues following Ala, Ile, Leu, Thr, and Val recorded using the pulse scheme of Figure 1a (measurement of $R_{3D_Z^2-2}$) with $T = 0.5$ ms. Only the correlations from A90 and I92 (^{1}H,^{15}N shifts at Y91 and Y93, respectively) which have very low intensities are not displayed at the threshold chosen. Many of the peaks are well isolated, so that ^{2}H relaxation rates can be obtained, illustrated in Figures 3a,b.

The ^{2}H spin relaxation rates are given by the following relations

$$R_{D_Z} = \frac{3}{40}\left(\frac{e^2qQ}{\hbar}\right)^2 [J(\omega_D) + 4J(2\omega_D)] \quad (3a)$$

$$R_{3D_Z^2-2} = \frac{3}{40}\left(\frac{e^2qQ}{\hbar}\right)^2 [3J(\omega_D)] \quad (3b)$$

$$R_{D_+} = \frac{1}{80}\left(\frac{e^2qQ}{\hbar}\right)^2 [9J(0) + 15J(\omega_D) + 6J(2\omega_D)] \quad (3c)$$

$$R_{D_+D_Z+D_ZD_+} = \frac{1}{80}\left(\frac{e^2qQ}{\hbar}\right)^2 [9J(0) + 3J(\omega_D) + 6J(2\omega_D)] \quad (3d)$$

where (e^2qQ/h) is the quadrupolar coupling constant (167 kHz used in what follows) and $J(\omega)$ is the spectral density function. Contributions from chemical exchange to the measured ^{2}H transverse magnetization decay rates can be neglected to excellent approximation because of the rapid decay of the magnetization from quadrupolar relaxation in this case. A particularly nice feature of the ^{2}H experiments is that it is possible to assess the consistency of the data on a per residue basis prior to the extraction of dynamics parameters, providing a measure of confidence in the data. Provided that $J(0) \geq J(\omega_D) \geq J(2\omega_D)$, Jacobsen et. al. have shown that the quadrupolar relaxation rates (eqs 3a−d) are related according to[38]

$$R_{D_Z} \leq \frac{5}{3}R_{3D_Z^2-2} \leq R_{D_+} \leq \frac{5}{3}R_{D_+D_Z+D_ZD_+} \quad (4)$$

Figures 3a and b show the four quadrupolar relaxation rates multiplied by the coefficients indicated in eq 4 as a function of residue in Δ131Δ, recorded at 600 and 500 MHz, respectively. No violation of the inequalities are observed in these two data sets. A second consistency relationship can be derived from eqs 3b−d

$$R_{D_+D_Z+D_ZD_+} = R_{D_+} - \frac{2}{3}R_{3D_Z^2-2} \quad (5)$$

Figures 3c and d illustrate the excellent agreement between $R_{D_+D_Z+D_ZD_+}$, R_{D_+}, and $R_{3D_Z^2-2}$ rates measured at both 600 and 500 MHz. This level of agreement is particularly noteworthy, given that the errors in rates are not insignificant (larger than for backbone relaxation data), because of the increased numbers of magnetization transfer steps in these experiments.

The deuterium relaxation rates were fitted using a spectral density function having the same form as eq 1 with S_f^2 replaced by $(^1/_9)S_{axis}^2$. Note that the factor of $^1/_9$ takes into account rotation about the methyl 3-fold axis so that the extracted order parameters reflect amplitudes of motion of the methyl averaging axis. As in fits of the ^{15}N relaxation data, τ_c^{eff} is allowed to vary on a per residue basis,[25] reflecting the fact that the motion at different side chains is likely to be quite diverse and anisotropic. Although the present model can only be considered crude at

(36) Davis, D. G.; Perlman, M. E.; London, R. E. *J. Magn. Reson., Ser. B* **1994**, *104*, 266−275.

(37) Mulder, F. A. A.; Hon, B.; Muhandiram, D. R.; Dahlquist, F. W.; Kay, L. E. *Biochemistry* **2000**, *39*, 12614−12622.

(38) Jacobsen, J. P.; Bildsoe, H. K.; Schaumburg, K. *J. Magn. Reson.* **1976**, *23*, 153−164.

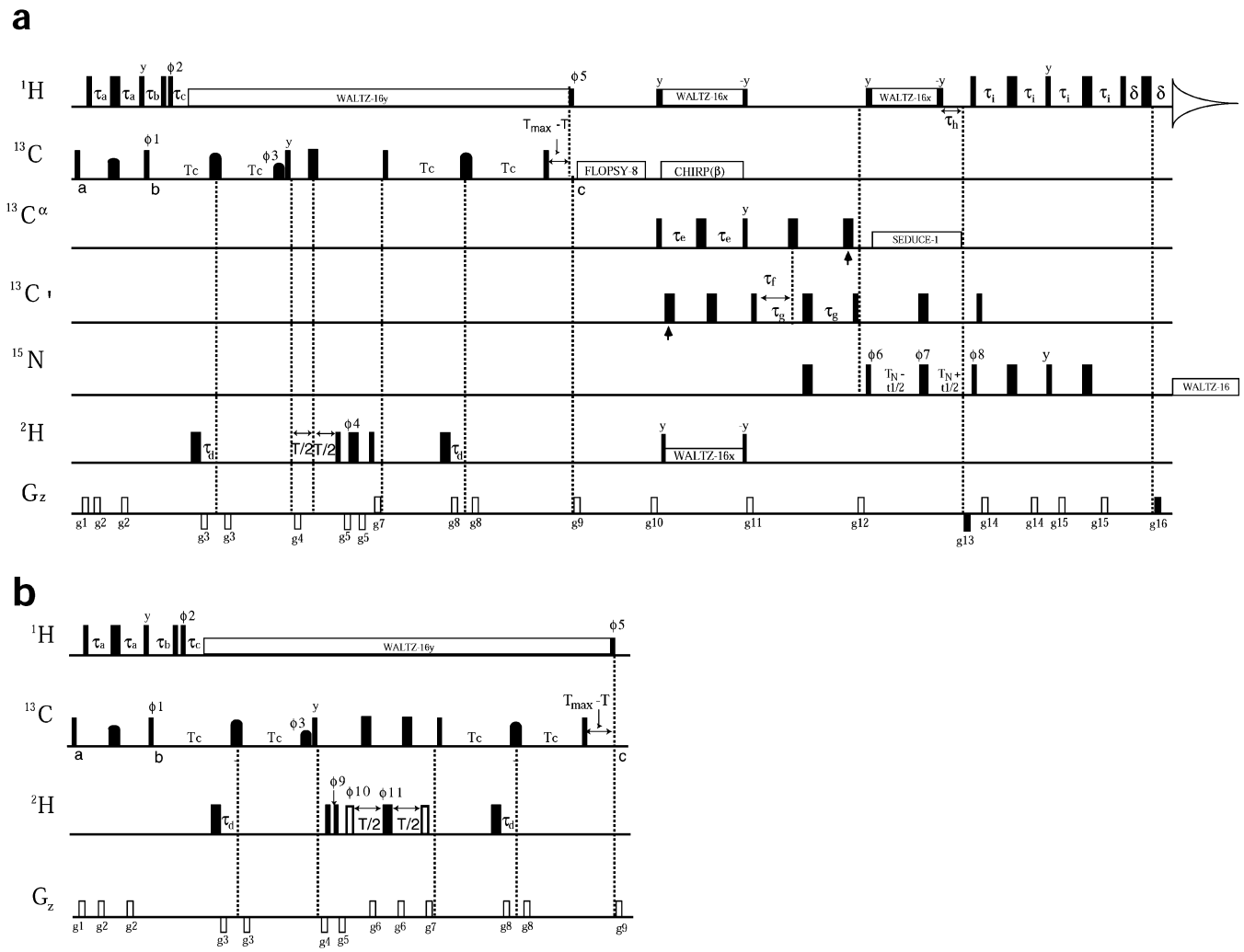

Figure 1. Pulse schemes used for the measurement of relaxation rates of deuterium quadrupolar order, $3D_Z^2 - 2$, $R_{3D_Z^2-2}$ (a), and antiphase transverse magnetization, $D_+D_Z + D_ZD_+$, $R_{D_+D_Z+D_ZD_+}$ (b), in unfolded protein states. Similar pulse schemes for the measurement of R_{D_Z} and R_{D_+} in unfolded proteins have been described previously[19] (minor modifications that have recently been incorporated are available from the authors upon request). All narrow (wide) rectangular pulses correspond to flip angles of 90° (180°) and are applied along the *x*-axis, unless otherwise indicated. Carriers are positioned at the water frequency (^1H), 119 ppm (^{15}N), 0.8 ppm (^2H, start of sequence until the end of the FLOPSY[65] mixing scheme), 4.7 ppm (^2H, immediately after FLOPSY mixing until the end of the sequence), 20 ppm (^{13}C, start of sequence until FLOPSY-8), 43 ppm (^{13}C FLOPSY mixing), and 58 ppm (^{13}C, immediately after the FLOPSY-8 until the end of the sequence). All proton pulses are applied with a 32.5 kHz field, with the exception of the 6.4 kHz field used for WALTZ decoupling[66] and the pulses immediately flanking the decoupling elements (also 6.4 kHz). The ^{13}C shaped 180° pulses between points a and b (1.36 ms at 600 MHz, centered at 19.5 ppm) and in the middle of the $2T_c$ periods (392 μs, 41 ppm) have RE-BURP profiles.[67] The ^{13}C pulse of phase $\phi3$ (640 μs, centered at 57 ppm) is applied with the SEDUCE-1 shape.[68] Magnetization relay through TOCSY mixing is achieved using the FLOPSY-8 scheme (8 kHz field, 7 cycles). $^{13}C_\beta$ decoupling fields, centered at both 29.5 ppm (±14.5 ppm) and 70.0 ppm (±2 ppm) and denoted by CHIRP(β), were implemented using a scheme comprised of 5 ms WURST-2 pulses.[69] The decoupling element was created using the Varian tool Pbox. All $^{13}C_\alpha$ rectangular pulses have durations which minimize excitation in the carbonyl region of the carbon spectrum and vice-versa.[70] Pulses indicated with vertical arrows are used to compensate for Bloch−Siegert effects.[71] $^{13}C_\alpha$ WALTZ decoupling during the constant time $2T_N$ period was achieved with 326 μs SEDUCE−1 pulses centered at 58 ppm. All ^{15}N pulses are applied with a 5.8 kHz field, with 1.1 kHz WALTZ-16 decoupling during acquisition. ^2H WALTZ decoupling employed a 0.7 kHz field; all other ^2H pulses are 2.0 kHz. The narrow rectangular pulses that are not filled in part b have flip angles of 45°. The delays employed are as follows: τ_a = 1.7 ms, τ_b = 3.85 ms, τ_c = 1.93 ms, T_c = 14.5 ms, τ_d = 1.7 ms, τ_e = 4 ms, τ_f = 4.4 ms, τ_g = 13.0 ms, τ_h = 5.5 ms, τ_i = 2.4 ms, T_N = 15 ms, and δ = 0.5 ms. T_{max} is chosen equal to the maximum value of T (relaxation delay) that is used in the relaxation series. The phase cycling is as follows: $\phi1$ = 2(*x*), 2(−*x*); $\phi2$ = *x*, −*x*; $\phi3$ = 4(*x*), 4(−*x*); $\phi4$ = 4(0°), 4(45°), 4(90°), 4(135°); $\phi5$ = −*x*, *x*; $\phi6$ = 16(*x*), 16(−*x*); $\phi7$ = 2(*x*), 2(−*x*); $\phi8$ = *x*; $\phi9$ = 4(*x*), 4(−*x*); $\phi10$ = 8(*x*), 8(−*x*); $\phi11$ = 16(*x*), 16(−*x*). For part a, rec. = *x*, 2(−*x*), *x*, −*x*, 2(*x*), −*x*, *x*, 2(−*x*), *x*, −*x*, 2(*x*), −*x*. After 16 scans, the phase of the receiver is inverted. For part b, rec. = *x*, 2(−*x*), 2(*x*), 2(−*x*), *x*, −*x*, 2(*x*), 2(−*x*), 2(*x*), −*x*. After 16 scans, the phase of the receiver is inverted. The durations and strengths of the gradients are g1 = (0.5 ms, 5 G/cm), g2 = (0.3 ms, 3 G/cm), g3 = (0.3 ms, −25 G/cm), g4 = (0.2 ms, −10 G/cm), g5 = (0.4 ms, −10 G/cm), g6= (0.05 ms, 25 G/cm), g7 = (0.25 ms, 6 G/cm), g8 = (0.2 ms, 10 G/cm), g9 = (0.6 ms, 15 G/cm), g10 = (1.0 ms, 15 G/cm), g11 = (0.4 ms, 6 G/cm), g12 = (0.5 ms, 25 G/cm), g13 = (1.25 ms, −30 G/cm), g14 = (0.2 ms, 2.5 G/cm), g15 = (0.3 ms, 2.0 G/cm), and g16 = (0.125 ms, 29.6 G/cm). Quadrature detection is achieved in t_1 using the enhanced sensitivity gradient approach,[72,73] with separate FIDs recorded for each t_1 point corresponding to ($\phi8$ = *x*, g13) and ($\phi8$ = −*x*, −g13). Decoupling is interrupted prior to the application of gradients.[74]

best, it is the simplest (in terms of numbers of parameters) that fits the data largely to within experimental error. Indeed, for 7 of 17 methyls reduced χ^2 values obtained from fits of rates using eqs 1 and 3 are less than 1, while for the remaining methyls χ^2 values less than 3 are obtained. It is noteworthy that fits of the rates to more complex spectral density functions with four fitting parameters[39] could not be justified on the basis of F-test statistical analyses (p values > 15% in all cases).

(39) Clore, G. M.; Szabo, A.; Bax, A.; Kay, L. E.; Driscoll, P. C.; Gronenborn, A. M. *J. Am. Chem. Soc.* **1990**, *112*, 4989−4991.

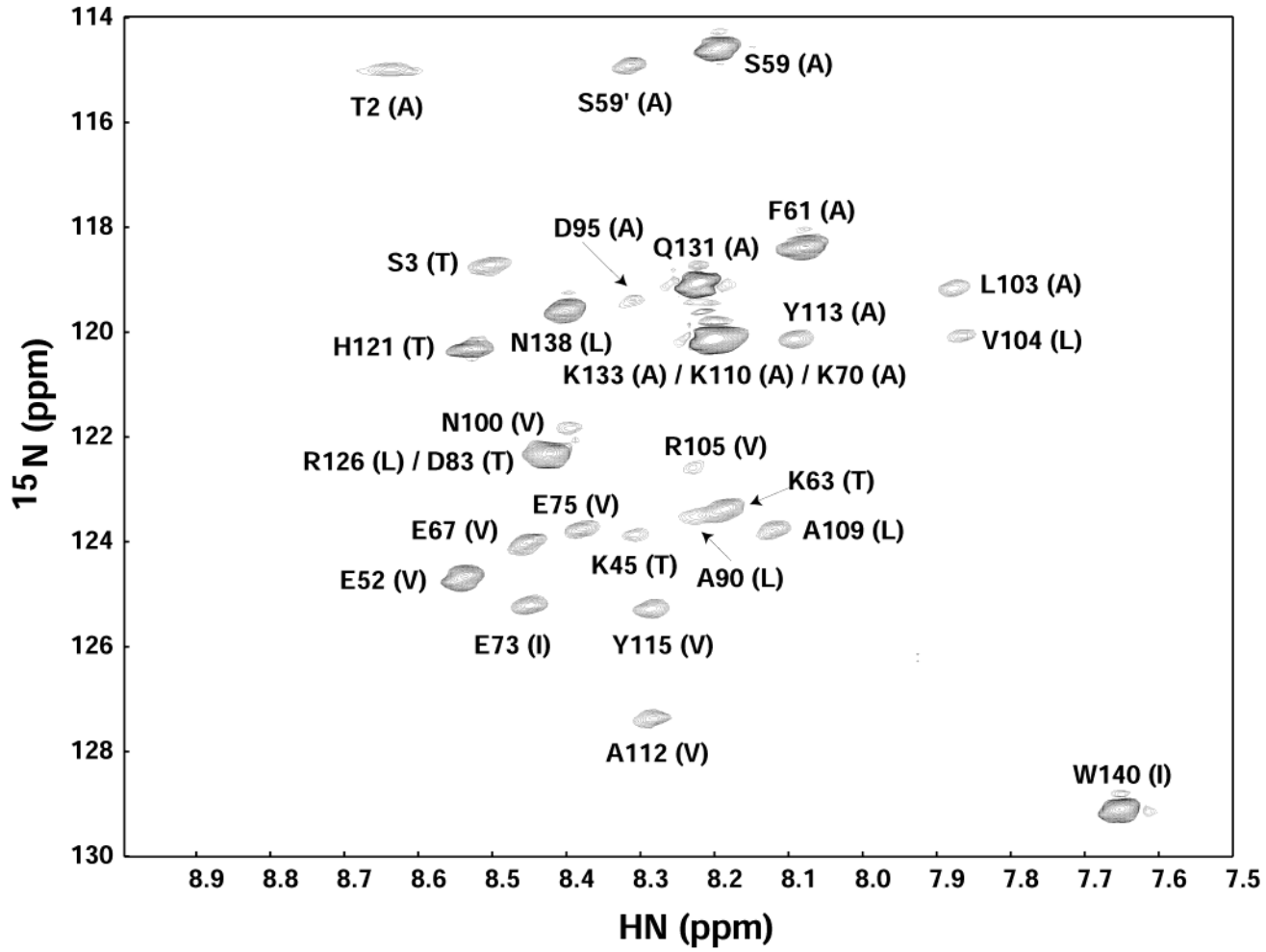

Figure 2. $^{1}H-^{15}N$ spectrum of Δ131Δ illustrating correlations from residues that immediately follow methyl-containing amino acids, recorded using the pulse scheme of Figure 2a (measurement of $R_{3D_Z^2-2}$ with $T = 0.5$ ms). The residue type from which magnetization originates is indicated in brackets beside each cross peak.

Thus, the simplest interpretation of the relaxation data is that the motion of a methyl can be described by an autocorrelation function which decays rapidly to a plateau value, followed by a more gradual decay with a rate that depends on internal slow (ns) time-scale dynamics and overall tumbling. That such a simple model fits the data is by no means proof that it describes accurately the nature of the side chain motions. Rather, the fits reflect the fact that, with a limited number of measurables, which, in turn, only probe the dynamics at specific frequencies, it is not possible to do better. The dynamics likely are more complicated and the extracted fitting parameters related in complex ways to the actual amplitudes and time scales of motion. This is important to keep in mind in general, but particularly so for studies of unfolded protein states where a superposition of a wide range of motions is likely involved.

As described previously, magnetization must be transferred from methyls to backbone amides for observation, and the motional parameters extracted are averages, therefore, over all methyls in a particular side chain. Simulations for Val and Leu residues have shown that for S^2_{axis} values at each methyl site between 0.2 and 0.8 the effective order parameter extracted deviates, on average, by 2.4% from the mean of the two. It is expected that the order parameters at both methyl sites in a Val or Leu will be very similar, since the methyls are "equidistant" from the backbone and are likely in a relatively unconstrained environment in the context of an unfolded protein. In the case of Ile, however, where both the dynamics at each methyl site and the transfer functions from the methyl carbons to the amides can be different, extracted S^2_{axis} values may be difficult to interpret.

Figure 4 shows the dynamics parameters obtained when the eight ^{2}H relaxation rates measured (four at each field) were fitted simultaneously, assuming a spectral density as in eq 1 with S^2_f replaced with $(^1/_9)S^2_{axis}$. As has been observed in fits of ^{15}N relaxation data of unfolded proteins, residue-specific values of τ_c^{eff} increase toward the middle of the molecule, reflecting the fact that overall dynamics are more constrained in the middle of an "unfolded" polypeptide chain than at the ends. The correlation times for the fast internal motions (τ_e) of the side chains range from 25 to 57 ps, with all except three between 41 and 57 ps. Values of τ_e are dominated by rapid methyl group rotations and are therefore not analyzed in any detail here.

Dynamics studies of a number of folded proteins indicate that despite the fact that backbone order parameters often show limited changes throughout the molecule, amplitudes of side chain motions can be quite heterogeneous.[1,40,41] A range of

(40) Flynn, P. F.; Urbauer, R. J. B.; Zhang, H.; Lee, A. L.; Wand, A. J. *Biochemistry* **2001**, *40*, 6559−6569.

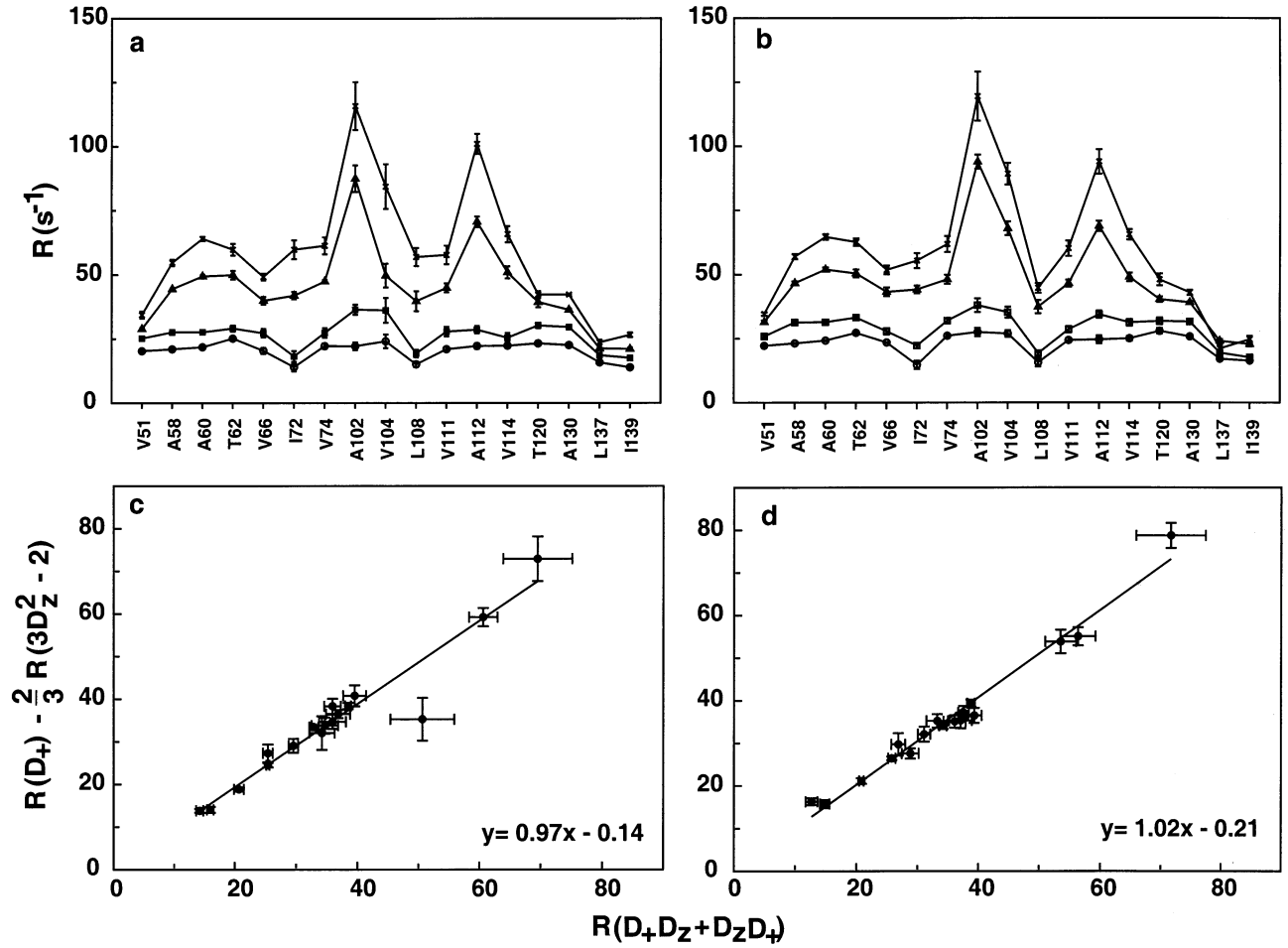

Figure 3. Plot of R_{D_Z} (○), $^5/_3R_{3D_Z^2-2}$ (□), R_{D_+} (△), and $^5/_3R_{D_+D_Z+D_ZD_+}$ (×) vs residue in Δ131Δ recorded at 600 MHz (a) and 500 MHz (b). All relaxation rates satisfy the inequality $R_{D_Z} \leq {}^5/_3R_{3D_Z^2-2} \leq R_{D_+} \leq {}^5/_3R_{D_+D_Z+D_ZD_+}$, as expected[38] for consistent data. In parts c and d, the consistency relation, $R_{D_+D_Z+D_ZD_+} = R_{D_+} - {}^2/_3R_{3D_Z^2-2}$ has been evaluated using experimentally measured deuterium relaxation rates at 600 and 500 MHz, respectively.

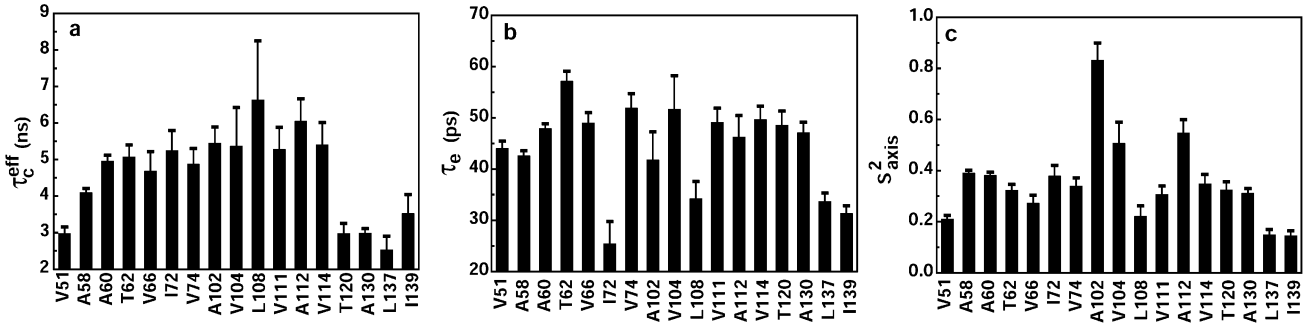

Figure 4. Motional parameters τ_c^{eff} (a), τ_e (b), and S^2_{axis} (c) derived from ^2H spin relaxation measurements vs residue. The Lipari−Szabo model-free approach[33,34] is employed in the analysis, as described in the text. The errors in each of the values are derived from 500 Monte Carlo simulations and are displayed on top of the bars.

S^2_{axis} values is observed for methyls in Δ131Δ, although, with the exception of A102, values are between ∼0.2−0.5 (Figure 4c), smaller than what is observed in folded proteins. Side chain order parameters are expected to decrease as the separation from the backbone increases because of the greater number of intervening torsion angles. To "correct" for the "intrinsic" differences of side chain order parameters between different amino acid types, average methyl axis order parameters (S^2_{DB}) for Ala, Val, Leu, Ile, and Thr have been extracted from a database of methyl axis order parameters compiled by Mittermaier et al.[42] For Val, Leu, and Ile, S^2_{DB} values are the averages over ($C_\beta-C_{\gamma 1}$, $C_\beta-C_{\gamma 2}$), ($C_\gamma-C_{\delta 1}$, $C_\gamma-C_{\delta 2}$), and ($C_\beta-C_{\gamma 2}$, $C_{\gamma 1}-C_\delta$) order parameters in the database, respectively.

Figure 5 shows that there is a reasonable correlation between S^2_{axis} and S^2_{NH} values for methyl-containing residues in Δ131Δ (a) and that this correlation improves, not surprisingly, when S^2_{axis} is "corrected" for the length of the side chain (b). (Note that as the degree of motion of a given methyl increases, S^2_{axis}

(41) Liu, W.; Flynn, P. F.; Fuentes, E. J.; Kranz, J. K.; McCormick, M.; Wand, A. J. *Biochemistry* **2001**, *40*, 14744−14753.

(42) Mittermaier, A.; Kay, L. E.; Forman-Kay, J. D. *J. Biomol. NMR* **1999**, *13*, 181−185.

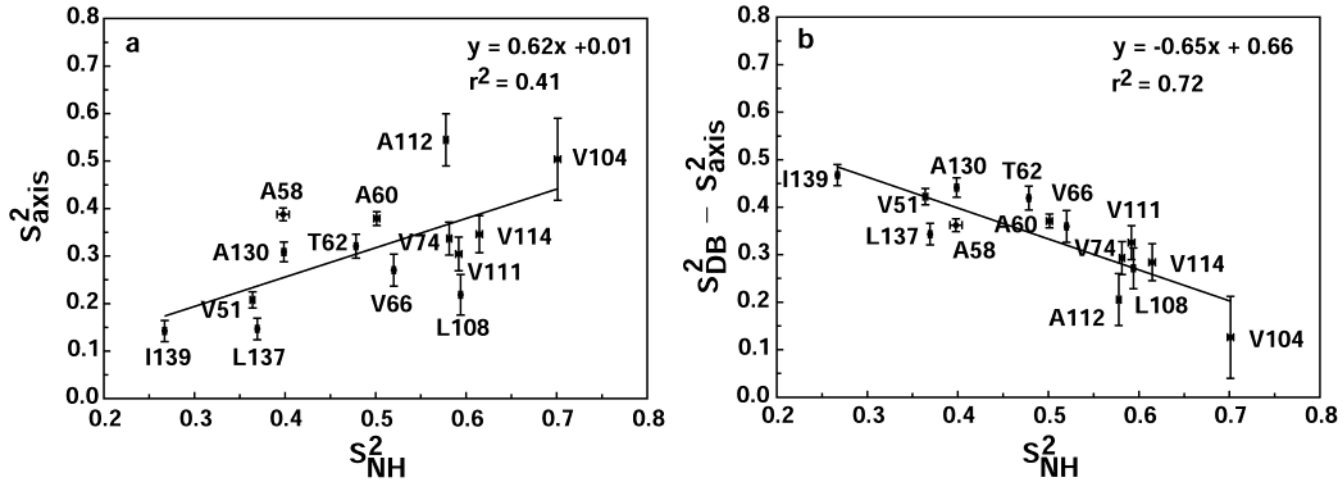

Figure 5. (a) Plot of order parameters of methyl symmetry axes (S^2_{axis}) vs backbone $^1H-^{15}N$ order parameters (S^2_{NH}). The S^2_{axis} of Val, Leu, and Ile are the averaged values of ($C_\beta-C_{\gamma1}$, $C_\beta-C_{\gamma2}$), ($C_\gamma-C_{\delta1}$, $C_\gamma-C_{\delta2}$), and ($C_\beta-C_{\gamma2}$, $C_{\gamma1}-C_\delta$) bonds, respectively. (b) Plot of $S^2_{DB} - S^2_{axis}$ versus S^2_{NH}, where S^2_{DB} is the averaged side chain order parameter for a given amino acid extracted from the database compiled by Mittermaier et al.[42] S^2_{DB} equals 0.75, 0.61, 0.49, 0.74, and 0.63 for Ala, Ile, Leu, Thr, and Val, respectively.

decreases while $S^2_{DB} - S^2_{axis}$ increases, so that the slopes of the correlations indicated in Figure 5a and b are of opposite sign).

Relating S^2_{axis} for Val and Thr to a Simple Motional Model. It is instructive to recast S^2_{axis} values for Val and Thr in terms of a model in which motion of the $C_\beta-C_\gamma$ bond is the sum of contributions from (i) backbone dynamics, (i.e., motion of the $C_\alpha-C_\beta$ bond) and (ii) χ_1 torsional angle fluctuations.[43−45] In what follows, we prefer not to interpret S^2_{axis} values from Ile residues, since, as described previously, these values are complex combinations of order parameters from both γ and δ methyl positions. In addition, S^2_{axis} values for Leu residues are not fit to a "physical" model of dynamics, since the number of experimental parameters is not sufficient in this case.

Figure 6 illustrates schematically the cone−Gaussian-axial-fluctuation (cone−GAF) model that has been chosen. The $C_\alpha-C_\beta$ bond wobbles uniformly in a cone with semiangle θ_o (step 1 in the Figure), with the $C_\beta-C_\gamma$ bond rotating about χ_1 (step 2). Thus, the distribution function, $p(\theta)$, describing the bond orientation in the cone is given by

$$p(\theta) = \text{constant for } 0° \le \theta \le \theta_o$$
$$= 0 \qquad \text{otherwise} \tag{6}$$

with θ_o related to the square of the order parameter describing the amplitude of the $C_\alpha-C_\beta$ bond vector motion, $S^2_{C\alpha-C\beta}$, according to[44,46]

$$S^2_{C\alpha-C\beta} = \frac{1}{4}\cos^2\theta_o*(1+\cos\theta_o)^2 \tag{7}$$

In the analysis of our data, we have substituted measured values of S^2_{NH} for $S^2_{C\alpha-C\beta}$. Molecular dynamics simulations and experimental data for folded proteins show that these order parameters are very similar in magnitude, with $S^2_{C\alpha-C\beta}$ values larger by approximately 0.06 units.[47,48]

Assuming independence of the wobbling in a cone and the χ_1 torsion angle fluctuations, we can derive an expression for S^2_{axis} analytically (see Appendix) as a function of θ_o and the standard deviation of the χ_1 torsion angle fluctuation (σ_{χ_1})

$$S^2_{axis} = S^2_{C\beta-C\gamma} = \left(\frac{1}{192}\right)$$
$$\left\{\begin{array}{l}\sin^4(\beta)\,(7+4\cos\theta_o+\cos^2\theta_o)^2\exp(-4\sigma^2_{\chi_1})+\\ \sin^2(2\beta)\,(1+7\cos\theta_o+4\cos^2\theta_o)^2\exp(-\sigma^2_{\chi_1})+\\ 12(3\cos^2(\beta)-1)^2(\cos\theta_o+\cos^2\theta_o)^2\end{array}\right\} \tag{8}$$

where $(180° - \beta)$ is equal to the $C_\alpha-C_\beta-C_\gamma$ bond angle. Table 1 lists σ_{χ_1} values derived from the cone−GAF model for the six Val and the one Thr for which both ^{15}N and ^2H relaxation data could be obtained. It is noteworthy that a 5% increase in the value of S^2_{NH} used to calculate θ_o, accounting for potential differences between S^2_{NH} and $S^2_{C\alpha-C\beta}$, translates into less than a 1° increase in calculated σ_{χ_1} values, on average. A second potential source of error derives from chemical exchange contributions to measured ^{15}N $R_{1\rho}$ rates, leading to an overestimation of S^2_{NH} and therefore σ_{χ_1}. On the basis of a B_1 field dependent study, we estimate an average contribution of approximately 5% to the ^{15}N transverse decay rates of the Val and Thr residues considered in Table 1, with a maximum contribution of 11% to Val 114. This translates into errors of no more than 1.1° in σ_{χ_1}.

A second related model has also been used to fit the relaxation data in which it is assumed that the distribution describing the wobbling of the $C_\alpha-C_\beta$ bond in a cone is Gaussian,[46,49] with $p(\theta)$ given by

$$p(\theta) = \frac{1}{\sqrt{2\pi\sigma^2_\theta}}\exp\left(\frac{-\theta^2}{2\sigma^2_\theta}\right) \tag{9}$$

where σ_θ is the standard deviation of the normal distribution of

(43) Richarz, R.; Nagayama, K.; Wuthrich, K. *Biochemistry* **1980**, *19*, 5189−5196.
(44) Brainard, J. R.; Szabo, A. *Biochemistry* **1981**, *20*, 4618−4628.
(45) Wittebort, R. J.; Szabo, A. *J. Chem. Phys.* **1978**, *69*, 1722−1736.
(46) Kinosita, K., Jr.; Ikegami, A.; Kawato, G. *Biophys. J.* **1982**, *37*, 461−464.
(47) Palmer, A. G.; Case, D. A. *J. Am. Chem. Soc.* **1992**, *114*, 9059−9067.
(48) Fadel, A. R.; Jin, D. Q.; Montelione, G. T.; Levy, R. M. *J. Biomol. NMR* **1995**, *6*, 221−226.
(49) Petersen, N. O.; Chan, S. I. *Biochemistry* **1976**, *16*, 2657−2667.

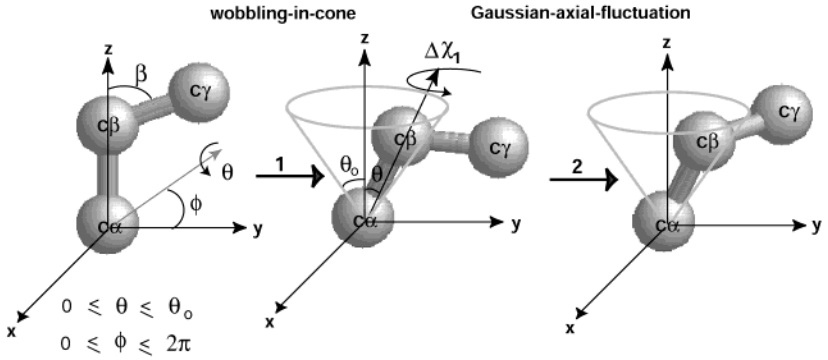

Figure 6. Schematic illustration of the averaging steps in the cone−GAF motional model. The $C_\alpha-C_\beta$ bond diffuses in a cone of semiangle θ_o (step 1). In addition, the $C_\beta-C_\gamma$ bond undergoes Gaussian axial fluctuations about its equilibrium position with standard deviation σ_{χ_1} (step 2).

Table 1. Cone Angle, θ_o, and Standard Deviation of χ_1 Fluctuations, σ_{χ_1}, for Val and Thr in Δ131Δ, Derived from the Cone−GAF Models[a]

	cone−GAF (model 1)[b]		cone−GAF (model 2)[c]	
residue	θ_o (deg)	σ_{χ_1} (deg)	σ_θ (deg)	σ_{χ_1} (deg)
V51	45.0 ± 0.1	37.4 ± 1.8	23.9 ± 0.1	37.2 ± 1.8
V66	36.8 ± 0.1	36.8 ± 3.1	19.1 ± 0.1	36.8 ± 3.1
V74	33.7 ± 0.1	33.1 ± 2.5	17.4 ± 0.1	33.0 ± 2.6
V104	27.5 ± 0.2	25.9 ± 4.9	14.0 ± 0.1	25.8 ± 4.9
V111	33.1 ± 0.2	36.0 ± 2.9	17.1 ± 0.1	35.9 ± 2.9
V114	32.0 ± 0.2	33.4 ± 2.8	16.4 ± 0.1	33.3 ± 2.8
T62	38.9 ± 0.1	31.2 ± 1.8	20.3 ± 0.1	31.1 ± 1.8

[a] Values are reported as mean ± standard deviation of 500 Monte Carlo simulations based on the mean values of S^2_{NH} and S^2_{axis} and their estimated standard deviations. [b] $C_\alpha-C_\beta$ bond wobbles in a restricted cone with semiangle equal to θ_o, eq 8. [c] $C_\alpha-C_\beta$ wobbles in a Gaussian cone, eq A9.

θ. Very similar amplitudes of χ_1 torsion angle fluctuations were obtained when data are fit using either eq 6 or 9 (Table 1).

Interpretation of σ_{χ_1} in the Context of an Unfolded State Ensemble. Unlike the folded state of a protein which can be well represented by a single structure, the unfolded state is an ensemble of fast interconverting conformers. The structural and dynamic properties that are observed, such as NOEs, scalar and dipolar couplings, and order parameters, for example, are ensemble-averaged quantities.[50] In the case at hand, the measured relaxation rates of coherences in an unfolded protein are obtained from single-exponential fits of magnetization that derive from all spins in the ensemble. To better interpret what the σ_{χ_1} parameters obtained in the case of an averaging system actually represent, we have carried out a number of simulations. In what follows, we have assumed that the spectral density function is given by eq 1 with S^2_f replaced by $(^1/_9)S^2_{axis}$ and that the cone−GAF model, eq 8, describes the side chain dynamics. It is possible to calculate both backbone ^{15}N and methyl deuterium relaxation rates for Val or Thr residues so long as the motional parameters S^2_{NH}, τ_c^{NH}, τ_e^{NH}, σ_{χ_1}, τ_c^{eff}, and $\tau_e^{C\beta-C\gamma}$, along with the population of each conformer in the unfolded state ensemble, are known.

A simulation was performed with an ensemble consisting of 100 different conformers which are assumed to interconvert with rates that are fast compared to both (i) any of the measured spin relaxation rates and (ii) chemical shift differences between states but are slow compared to $1/\tau_c^{NH}$. In this limit, each of the effective relaxation rates for the ensemble (R_{D_Z}, R_{D_+} ...) is given by the population weighted average of the rates. Conformer

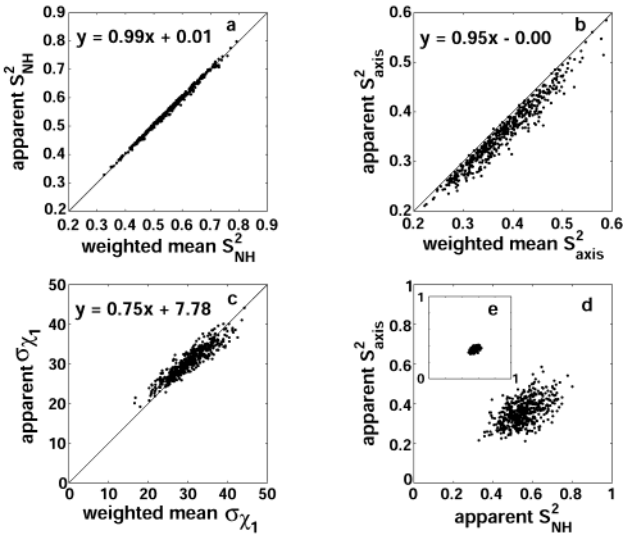

Figure 7. Plots of apparent S^2_{NH} vs population weighted mean S^2_{NH} values (a), apparent S^2_{axis} vs population weighted mean S^2_{axis} (b), apparent σ_{χ_1} vs population weighted mean σ_{χ_1} (c), and apparent S^2_{axis} vs apparent S^2_{NH} (d) obtained from simulations described in the text. The inset to part d shows results from an additional simulation, where the probabilities of all the ensemble elements are assumed to be equal (see Materials and Methods for details).

averaged S^2_{NH}, S^2_{axis}, and σ_{χ_1} values were subsequently extracted from fits of the rates, in the same manner as experimental values are obtained, and the process was repeated 500 times (i.e., 500 ensembles) to get a distribution of dynamics parameters (referred to as apparent order parameters in what follows). These distributions are compared with the corresponding population weighted mean values, Figure 7. Of note, the apparent and ensemble weighted mean σ_{χ_1} values are very close (Figure 7c) so that a simple interpretation of extracted σ_{χ_1} values from relaxation measurements is possible.

Figure 7d shows that there is a significant correlation between the apparent backbone and side chain order parameters, as observed experimentally (Figure 5). In addition, the range of order parameter values obtained by simulation corresponds well to the range observed experimentally. This is in contrast to the case, where simulations are performed assuming that each member of the ensemble is equiprobable, in which case a much smaller range of dynamics parameters are observed (Figure 7e). This result is consistent with what has been observed in previous studies of Δ131Δ that strongly support the fact that the ensemble is dominated by a small number of distinct conformers.[30,31]

(50) Choy, W. Y.; Forman-Kay, J. D. *J. Mol. Biol.* **2001**, *308*, 1011−1032.

Comparison of χ_1 Distributions in Folded and Unfolded Protein States. Fluctuations of χ_1 in folded proteins can be probed by measurement of a subset of the nine possible ^3J-coupling constants that are related to this torsion angle.[51−56] Recently, West and Smith have parametrized the Karplus equation for the $^3J_{H\alpha H\beta}$-coupling constant on the basis of data from 138 residues in 10 folded proteins.[55] The Karplus equation so generated was then compared to those reported by de Marco et al.[57] and Kopple et al.,[58] obtained from measurements on rigid cyclic compounds, where χ_1 averaging should be very minimal. On the basis of this comparison, the average standard deviation of the χ_1 torsion angle fluctuations in the 10 proteins considered was found to be 26°. This extent of motion is comparable to that found for dynamics of the ϕ torsion angle in protein cores.[54]

Schmidt and co-workers have proposed a self-consistent ^3J-coupling analysis protocol which makes use of a large set of independent coupling constants related to a single torsion angle. Initial estimates of all involved Karplus coefficients can be refined using this procedure, and local angular mobility can be determined on the basis of Gaussian axial fluctuation or rotameric jump models.[56] In an application to the protein *D. vulgaris* flavodoxin, this group determined that the standard deviations of Gaussian fluctuations of χ_1 (σ_{χ_1}) for different residues varies from 0.0 to 48.6°, with a mean of 24.4°. The nine Val residues in this protein show a more narrow range of χ_1 mobility ($\sigma_{\chi_1} = 15.8°-30.7°$), but with a mean σ_{χ_1} also equal to 24.4°. Of interest, using the database of side chain dynamics parameters for folded proteins obtained by ^{2}H spin relaxation measurements,[42] we have calculated using the cone−GAF model that for Val $\sigma_{\chi_1} = 19.9 \pm 10.6°$. For Δ131Δ, the average σ_{χ_1} for the six Val residues for which data are available is 33.8°, larger than what is observed for folded proteins. Larger values for unfolded protein states are not unexpected, since these systems are significantly more dynamic than their folded counterparts. However, larger values could also be the result of the fact that S^2_{axis} values are sensitive to both dynamics within a well (corresponding to torsion angle fluctuations from $\chi_1 + \Delta\chi$ to $\chi_1 - \Delta\chi$) and jumps between wells. Detailed simulations have established that S^2_{axis} values from ^{2}H spin relaxation experiments are sensitive to such jumps if they occur with correlation times smaller than about 2 ns. The fact that very similar σ_{χ_1} values are obtained for folded proteins from scalar couplings and ^{2}H spin relaxation suggests, however, that, at least for folded molecules, rotameric jumps may well occur with time constants larger than 2 ns.

Conclusions

In this paper, we have presented a new set of pulse schemes for the study of methyl-containing side chain dynamics in partially unfolded and unfolded protein states. Methyl side chain dynamics in an unfolded protein deletion mutant, Δ131Δ, have been studied, and a high correlation between backbone and side chain order parameters observed. This correlation is distinct from that commonly found in folded proteins. A cone−GAF model has been proposed to estimate the amplitude of χ_1 torsion angle fluctuations for Val and Thr on the basis of backbone and side chain order parameters. The average σ_{χ_1} value for the six Val residues for which data could be obtained is 33.8°, approximately 10° larger than for folded proteins using either ^3J-coupling constants or ^{2}H spin relaxation as probes. This indicates, not surprisingly, that side chains of unfolded protein states are distinctly more dynamic than in folded proteins. Of note, however, is the value of σ_{χ_1} for Val 104 which is considerably smaller than those for other residues, suggesting that it may be part of a hydrophobic cluster. The present work lays the foundation for extracting more detailed structural information about unfolded state ensembles from side chain dynamics data.

Materials and Methods

All spin relaxation experiments were recorded on a 3.2 mM ^{15}N,^{13}C,50% ^{2}H-labeled sample of Δ131Δ, 1 mM sodium azide, pH 5.1, $T = 32$ °C. Details of sample preparation are as given previously[26] with the exception that the protein was expressed in media containing 50% D_2O.

Deuterium Relaxation Measurements. Deuterium spin relaxation experiments were recorded on Varian Inova 600 and 500 MHz spectrometers as complex data matrices comprised of 48 × 576 points (600 MHz) or 40 × 512 points (500 MHz). 48 (64) transients/FID were signal averaged in the measurement of R_{D_z} and R_{D_+} at 600 (500) MHz, while 96 (128) scans were recorded for $R_{3D_Z{}^2-2}$ and $R_{D_+D_Z+D_ZD_+}$. Delays between scans of 1.5 s were employed. For $R_{D_Z}(R_{3D_Z{}^2-2})$ experiments, the variable delay T (see Figure 1) was incremented from 0.5 to 40 ms (0.5−50 ms), while, for R_{D_+} and $R_{D_+D_Z+D_ZD_+}$, delays ranged from 0.5 to 30 ms.

All data sets were processed and analyzed with NMRPipe software.[59] Rates were obtained by fitting cross-peak intensities to a single exponential function with errors estimated by Monte Carlo analysis.[60] Motional parameters, S^2_{axis}, τ_c^{eff}, and τ_e were extracted by minimizing a function of the form $\chi^2 = \sum_i (R_{i,calc} - R_{i,expt})^2/\sigma_i^2$, where $R_{i,calc}$ and $R_{i,expt}$ are the calculated and experimental relaxation rates, the index i labels each of the eight independent relaxation rates measured (4 rates/field), and σ_i is the estimated error in experimental relaxation rate "i" obtained from Monte Carlo analysis. Expressions for $R_{i,calc}$ are given in eq 3 using the form of spectral density function defined by eq 1 with S_f^2 replaced by $(^1/_9)S^2_{axis}$.

Backbone ^{15}N Relaxation Measurements. T_1, $T_{1\rho}$, and ^{1}H−^{15}N NOE experiments[61] were recorded at 32 °C on a Varian Inova 600 MHz spectrometer. T_1 experiments were performed with 8 relaxation delays T varying from 10 to 800 ms, while $T_{1\rho}$ experiments[62] were recorded with 8 relaxation delays between 10 and 100 ms. Steady-state ^{1}H−^{15}N NOE values were determined from spectra recorded in the presence and absence of proton saturation. NOE spectra recorded with proton saturation utilized a 7 s relaxation delay followed by a 5 s period of saturation, while spectra recorded in the absence of proton saturation employed a relaxation delay of 12 s.

All T_1, $T_{1\rho}$, and ^{1}H−^{15}N NOE spectra were recorded as 128 × 615 complex matrices with spectral widths of 9611.9 and 1350 Hz in the

(51) Hoch, J. C.; Dobson, C. M.; Karplus, M. *Biochemistry* **1985**, *24*, 3831−3841.
(52) Dzakula, Z.; Westler, W. M.; Edison, A. S.; Markley, J. L. *J. Am. Chem. Soc.* **1992**, *114*, 6195−6199.
(53) Karimi-Nejad, Y.; Schmidt, J. M.; Ruterjans, H. *Biochemistry* **1994**, *33*, 5481−5492.
(54) Bruschweiler, R.; Case, D. A. *J. Am. Chem. Soc.* **1994**, *116*, 11199−11200.
(55) West, N. J.; Smith, L. J. *J. Mol. Biol.* **1998**, *280*, 867−877.
(56) Perez, C.; Lohr, F.; Ruterjans, H.; Schmidt, J. M. *J. Am. Chem. Soc.* **2001**, *123*, 7081−7093.
(57) de Marco, A.; Llinas, M.; Wuthrich, K. *Biopolymers* **1978**, *17*, 617−636.
(58) Kopple, K. D.; Wiley: G. R.; Tauke, R. *Biopolymers* **1973**, *12*, 627−636.
(59) Delaglio, F.; Grzesiek, S.; Vuister, G. W.; Zhu, G.; Pfeifer, J.; Bax, A. *J. Biomol. NMR* **1995**, *6*, 277−293.
(60) Kamith, U.; Shriver, J. W. *J. Biol. Chem.* **1989**, *264*, 5586−5592.
(61) Farrow, N. A.; Muhandiram, D. R.; Singer, A. U.; Pascal, S. M.; Kay, C. M.; Gish, G.; Shoelson, S. E.; Pawson, T.; Forman-Kay, J. D.; Kay, L. E. *Biochemistry* **1994**, *33*, 5984−6003.
(62) Korzhnev, D. M.; Skrynnikov, N. R.; Millet, O.; Torchia, D. A.; Kay, L. E. *J. Am. Chem. Soc.* **2002**, *124*, 10743−10753.

^1H and ^{15}N dimensions, respectively. R_1 and $R_{1\rho}$ values were obtained by fitting cross-peak intensities to a single exponential function with errors estimated by Monte Carlo analysis. R_2 values were extracted from $R_{1\rho}$ rates, as described previously.[36] Errors in NOE values were estimated on the basis of signal-to-noise in spectra recorded with and without proton saturation. Motional parameters, S^2_{NH}, τ_c^{NH}, and τ_e^{NH}, were extracted on a per residue basis by minimizing a function of the form

$$\chi^2 = (\sum_i (R_{i,calc} - R_{i,expt})^2/\sigma_i^2) + (NOE_{calc} - NOE_{expt})/\sigma^2_{NOE}$$

Ensemble Simulation. A simulation was performed to evaluate the relation between the order parameters extracted from the relaxation measurements (referred to as *apparent* S^2 values in what follows) and the corresponding population weighted average order parameters. A total number of 500 ensembles were generated, each consisting of 100 conformers. Each of the 100 conformers per ensemble is assumed to interconvert with rates that are fast compared to any of the measured spin relaxation rates and chemical shift differences between states but slow compared to $1/\tau_c^{NH}$. For each ensemble, random values of motional parameters were assigned to each conformer (i.e., each conformer fluctuates on a picosecond−nanosecond time scale). Values of dynamics parameters S^2_{NH} ranged from 0.1 to 1, τ_c^{NH} from 2 to 9 ns, and τ_e^{NH} from 50 to 250 ps; τ_c^{eff} was between 1 and τ_c^{NH} ns, and $\tau_e^{C\beta-C\gamma}$ ranged from 20 to 90 ps. All values were chosen with uniform probabilities. σ_{χ_1} values were chosen from a normal distribution centered at 30° with a standard deviation of 15°. Random but uneven populations, p_i, were assigned to each of the 100 molecules, $\Sigma_{i=1,100}\ p_i = 1$. The population for the first of the 100 conformers was randomly selected from 0 to 0.25. Subsequently, the population of each successive conformer was randomly assigned a value between 0 and 0.25 of the remaining population. In this manner, a skewed population distribution is obtained, dominated by a relatively small number of conformers. Side chain ^2H and backbone ^{15}N relaxation rates were calculated for each of the 500 ensembles as the population weighted average of the rates for each member of the ensemble according to R(ensemble j) = $\Sigma\ p_iR_i$, where R_i is the decay rate (R_{Dz}, R_{D+} ...) for conformer i ($1 \le i \le 100$) and $1 \le j \le 500$. Apparent S^2_{NH}, S^2_{axis}, and σ_{χ_1} values are obtained from fits of the R(ensemble j) values in a manner analogous to the extraction of motional parameters from the experimentally determined rates. For each ensemble, weighted mean values of these parameters are also calculated; for example, *weighted mean* $\sigma_{\chi_1} = \Sigma\ p_i\sigma^i_{\chi_1}$, where the set of all $\sigma^i_{\chi_1}$ values ($i = 1-100$) are those that have been randomly assigned to each of the conformers. Correlations between apparent and weighted mean values obtained for each ensemble are plotted in Figure 7. Note that a given value of σ_{χ_1} can be consistent with different motional models. For example, similar S^2_{axis} values are obtained for (i) a model in which rapid (time constants less than 2 ns, see Results and Discussion) jumps between each of the three canonical χ_1 states with populations and σ_{χ_1} values of 0.8, 20° ($\chi_1 = 60°$), 0.1, 15° ($\chi_1 = 180°$), and 0.1, 15° ($\chi_1 = 300°$) and for (ii) a model in which motion is confined to a single well with a σ_{χ_1} value of ∼35° (assuming $S^2_{NH} = 0.8$ in each case).

Acknowledgment. Dr. Oscar Millet (University of Toronto) and Dr. Nikolai Skrynnikov (Purdue University) are thanked for many useful discussions. W.-Y.C. is a recipient of a Senior Research Fellowship from the Canadian Institutes of Health Research (CIHR). This research was supported by a grant from the CIHR. L.E.K. holds a Canada Research Chair in Biochemistry.

Appendix

Cone−GAF Model Describing the Dynamics of the C_β−C_γ Bond Vector. The square of the order parameter of bond vector υ, S^2_υ, can be expressed as[33]

$$S^2_\upsilon = \frac{4\pi}{5}\sum_{m=-2}^{m=2}\langle Y_{2m}(\Omega^{lab}_\upsilon)\rangle\langle Y^*_{2m}(\Omega^{lab}_\upsilon)\rangle \qquad (A1)$$

where $Y_{2m}(\Omega)$ is a second-order rank-two spherical harmonic, Ω^{lab}_υ is the set of polar angles describing the orientation of bond vector υ in the laboratory frame, and the angular brackets indicate time averaging. The $\langle Y_{2m}(\Omega^{lab}_\upsilon)\rangle$ terms can be expressed as linear combinations of second-order spherical harmonics in the molecular frame,[63] so that

$$\langle Y_{2m}(\Omega^{lab}_\upsilon)\rangle = \sum_{p=-2}^{p=2} Y_{2p}(\Omega^{mol}_\upsilon)\langle D_{pm}(\alpha,\beta,\gamma)\rangle \qquad (A2)$$

where $D_{pm}(\alpha,\beta,\gamma)$ values are the p,m elements of the Wigner rotation matrix which transforms the molecular frame to the laboratory frame and (Ω^{mol}_υ) values are the polar angles of the bond vector in the molecular frame. In what follows, the z-axis of the molecular frame is chosen to lie along the $C_\alpha-C_\beta$ bond vector, and the $D_{pm}(\alpha,\beta,\gamma)$ elements, which describe the combined motion of wobbling in a cone and the Gaussian axial fluctuations about the $C_\alpha-C_\beta$ bond, can be expressed as

$$\langle D_{pm}(\alpha,\beta,\gamma)\rangle = \langle D_{pm}(\phi - \Delta\chi_1, -\theta, -\phi)\rangle = \langle e^{-ip(\phi-\Delta\chi_1)} d_{pm}(-\theta)e^{im\phi}\rangle \qquad (A3)$$

where θ and ϕ are the polar angles describing the orientation of the instantaneous $C_\alpha-C_\beta$ bond vector in the cone and $\Delta\chi_1$ is the χ_1 fluctuation about the $C_\alpha-C_\beta$ bond from the equilibrium position. Assuming that the χ_1 fluctuations are independent of the wobbling motion and substituting A3 into A2, we obtain

$$\langle Y_{2m}(\Omega^{lab}_\upsilon)\rangle = \sum_{p=-2}^{p=2} Y_{2p}(\Omega^{mol}_\upsilon)\langle e^{-i(p-m)\phi}\rangle\langle e^{ip\Delta\chi_1}\rangle\langle d_{pm}(-\theta)\rangle \qquad (A4)$$

where

$$\langle e^{-i(p-m)\phi}\rangle = \frac{1}{2\pi}\int_0^{2\pi} e^{-i(p-m)\phi}\,d\phi = \delta_{pm} \qquad (A5)$$

Therefore

$$\langle Y_{2m}(\Omega^{lab}_\upsilon)\rangle = Y_{2m}(\Omega^{mol}_\upsilon)\langle d_{mm}(-\theta)\rangle\langle e^{im\Delta\chi_1}\rangle \qquad (A6)$$

where

$$\langle d_{mm}(-\theta)\rangle = \frac{\int_0^{\theta_o} d_{mm}(-\theta)\sin(\theta)\,d\theta}{\int_0^{\theta_o}\sin(\theta)\,d\theta} \qquad (A7)$$

and

$$\langle e^{im\Delta\chi_1}\rangle = \int_{-\pi}^{\pi}\frac{1}{\sqrt{2\pi\sigma^2_{\chi_1}}}\exp(-(\Delta\chi_1)^2/2\sigma^2_{\chi_1})e^{im\Delta\chi_1}\,d\Delta\chi_1 \qquad (A8)$$

Bruschweiler and Wright have shown that the right-hand side of equation A8 is equal to $e^{-m^2\sigma_{\chi_1}{}^2/2}$ when $\sigma^2_{\chi_1}$, the variance of the Gaussian fluctuation about χ_1 (i.e., the $C_\alpha-C_\beta$ bond), is

(63) Zare, R. *Angular momentum*; Wiley-Interscience: New York, 1988.

sufficiently small ($\sigma_{\chi_1} \ll \pi$).[64] Substituting eqs A6−A8 into eq A1 gives eq 8 of the text.

In the case where the probability distribution function describing the diffusion of the $C_\alpha-C_\beta$ bond vector in the cone is also Gaussian, eq A7 is modified to[49]

$$\langle d_{mm}(-\theta)\rangle = \frac{\int_0^\pi \frac{1}{\sqrt{2\pi\sigma_\theta^2}} \exp(-\theta^2/2\sigma_\theta^2) d_{mm}(-\theta)\sin(\theta)\, d\theta}{\int_0^\pi \frac{1}{\sqrt{2\pi\sigma_\theta^2}} \exp(-\theta^2/2\sigma_\theta^2)\sin(\theta)\, d\theta} \quad \text{(A9)}$$

which can be solved numerically.

Supporting Information Available: One figure showing backbone ^{15}N dynamics parameters of Δ131Δ at 600 MHz. This material is available free of charge via the Internet at http://pubs.acs.org.

JA021179B

(64) Bruschweiler, R.; Wright, P. E. *J. Am. Chem. Soc.* **1994**, *116*, 8426−8427.
(65) Mohebbi, A.; Shaka, A. J. *J. Chem. Phys.* **1991**, *178*, 374−377.
(66) Shaka, A. J.; Keeler, T.; Fenkiel, T.; Freeman, R. *J. Magn. Reson.* **1983**, *52*, 335−338.
(67) Geen, H.; Freeman, R. *J. Magn. Reson.* **1991**, *93*, 93−141.
(68) McCoy, M.; Mueller, L. *J. Am. Chem. Soc.* **1992**, *114*, 2108−2110.
(69) Kupce, E.; Freeman, R. *J. Magn. Reson., Ser. A.* **1995**, *115*, 273−276.
(70) Kay, L. E.; Ikura, M.; Tschudin, R.; Bax, A. *J. Magn. Reson.* **1990**, *89*, 496−514.
(71) Vuister, G. W.; Bax, A. *J. Magn. Reson.* **1992**, *98*, 428−435.
(72) Kay, L. E.; Keifer, P.; Saarinen, T. *J. Am. Chem. Soc.* **1992**, *114*, 10663−10665.
(73) Schleucher, J.; Sattler, M.; Griesinger, C. *Angew. Chem., Int. Ed. Engl.* **1993**, *32*, 1489−1491.
(74) Kay, L. E. *J. Am. Chem. Soc.* **1993**, *115*, 2055−2056.